TRANSACTIONS OF THE INSTITUTE OF FLUID-FLOW MACHINERY

No. 138, 2017, 107–123

Sebastian Kornet*, Mariusz Banaszkiewicz, Janusz Badur

Numerical analysis of the onset of condensation in the IMP PAN nozzle for cases without the appearance of shock waves in the steam flow

Energy Conversion Department, Institute of Fluid-Flow Machinery, Polish Academy of Sciences, Fiszera 14, 80-231 Gdańsk, Poland

Abstract

The present paper focuses on the prediction of the spontaneous condensation phenomena in the wet steam flow depending on the inlet temperature. The basic tests including comparison with experimental data have been performed using the planar symmetrical nozzle with the de Laval geometry (IMP PAN nozzle). It was assumed in calculations that steam is pure and does not contain heterogeneous sources of condensation. Numerical analysis was performed for boundary conditions which correspond to the flow regime without the shock wave. The present work includes simulations results of the onset of condensation and shows whether initiation of phase transition is located in the region between a spinodal and a binodal. Numerical results along the nozzle axis are presented on thermodynamic diagrams for all considered flow conditions.

Keywords: Spinodal, Binodal, Spontaneous condensation, SCWS model, IMP PAN nozzle, Wilson line

1 Introduction

Condensation phenomena and growth of droplets in supersonic expansions occur in a number of natural and technological processes, such as formation of aerosols, the flight of aircraft in humid conditions, droplet-spray combustion processes, in

*Corresponding Author. Email adress: skornet@imp.gda.pl

a phase separation devices or wet steam flows in steam turbines [1]. At the dawn of the 21stcentury it is still the case that the steam turbine remains an important component for the efficient production of energy in the power industry. Majority of the world's electricity generators are driven just by steam turbines [2].

For a single reheat cycle, the steam from the boiler flows to the high-pressure turbine where it expands and is exhausted back to the boiler for reheating. The reheat steam coming from the boiler flows to the intermediate-pressure turbine where it expands and exhausts into a crossover line that supplies the steam to the low-pressure turbine. The steam expands through low-pressure turbine and exhaust to a condenser. During the expansion process of steam in the low-pressure turbine the flow first supercools and then nucleates thus generating a large number of very small droplets to form a two-phase mixture (usually in the turbine last stage). The formation and evolution of these droplets lowers the performance of the turbine wet stages and their effect on the efficiency are commonly known as wetness losses. Thermodynamic irreversible losses, generated within the non-equilibrium conditions and phase change, are significant to the low-pressure stage efficiency since for every additional percent of wetness the efficiency is reduced by approximately 1%. In conventional power plants the wetness levels in last stages of the low-pressure turbine can be as high as 10–12%. In nuclear power plants exhaust wetness may reach 18% [3–11].

Owing to the early introduction of the de Laval nozzle (1883) into the steam turbine design, condensation investigations in a converging-diverging steam nozzle have been made for a long time. Laval nozzles have been used extensively to examine condensation of both mixtures of condensable vapor in carrier gas and pure vapors, especially steam. In de Laval nozzles, the cross-sectional flow area first decreases to the throat and then increases monotonically in the supersonic region [1,12].

According to Stodola [15] and other pioneers, rapid expansion of steam from superheated to wet condition in a typical convergent-divergent nozzle is illustrated in Fig. 1. Steam enters the nozzle as dry superheated vapor at point (1) and during its passage through the nozzle throat expands to the sonic condition represented by point (2). Between points (1) and (2) the steam cools down and the flow accelerates. At point (3) there is some theoretical possibility for the onset of an equilibrium phase transition governed mainly by Clapeyron-Clausius equation which can be virtually evaluated in numerical simulations. For the equilibrium approach one can calculate the equilibrium wetness and the equilibrium pressure, Fig. 1, [13–17]. At point (3) the expansion line crosses the saturation line ('dryness fraction', $x = 1$) on the Mollier enthalpy–entropy diagram. Then,

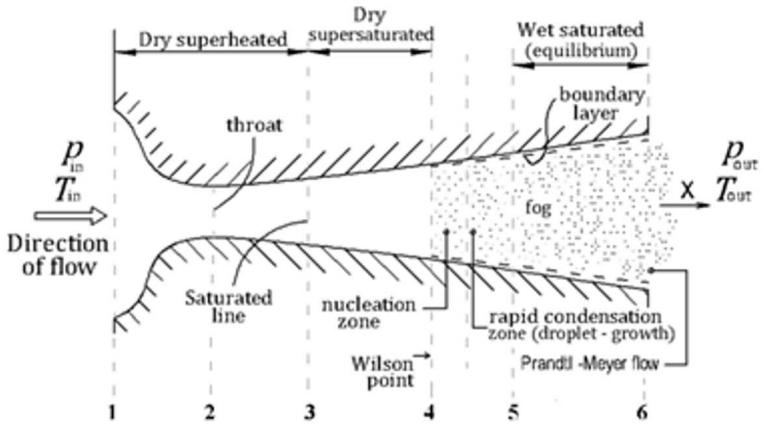

Figure 1: Characteristic events in condensing de Laval nozzle [17].

the steam is below the saturation conditions in a state called 'metastable', usually referred to as supercooled or supersaturated (between spinodal and binodal line). The nucleation rates associated with these early nuclei are so low that the steam continues to expand as a dry single phase vapor in a metastable, supercooled or supersaturated state. But after the limiting (critical) values of supercooling and supersaturation are reached the power of random fluctuations of kinetic motion of molecules is equal to the Gibbs work of creation of stable microclusters which are called the condense nucleation. Depending on the local conditions and the rate of expansion, the nucleation rate increases dramatically and reaches its maximum at point (4). Depending on the expansion rate, that change in the vicinity of point (4) from 10^3 s^{-1} to 10^5 s^{-1}, the rate of nucleation of new nuclei per unit of volume is huge and reaches even 10^{18} droplets per cubic meter. This process is termed 'homogeneous nucleation' or 'spontaneous nucleation'. The area is termed 'nucleation zone' and is terminated by the Wilson point (also known as 'inception point' or 'onset point'), which is the point of maximum supercooling level. Supercooling level, ΔT , is defined as the difference between the saturation temperature, $T_{sat}(p)$ at local pressure p , and the actual vapor temperature T_v [13–17]:

$$\Delta T = T_{sat}(p) - T_v \ . \tag{1}$$

In the case of steam, supercooling levels of approximately 40 K are achievable, while the steam still remains dry [1,2,10]. Downstream of point (4), nucleation ceases effectively and the number of droplets in the flow remains constant. The

nuclei grow rapidly between points (4) and (5) and restore the system to thermodynamic equilibrium. Further expansion of the flow between points (5) and (6) takes place close to equilibrium conditions [13–17].

Nucleation is practically terminated at the point of maximum subcooling called the Wilson point. For pure steam, if the Wilson points for tests with varying nozzle inlet conditions are plotted on the equilibrium Mollier diagram, they are contained within a narrow zone around a line called the Wilson line (which corresponds to approximately 3–4% equilibrium wetness line) [3,10,18]. In reality the position of this point depends on many parameters like pressure, temperature and expansion rate [11].

Several observations confirm that condensation often occurs earlier than it is predicted by theory, i.e., before the Wilson line. It is because the nucleation can start at some soluble and insoluble impurities, particles of dust, chemical compounds or corrosion products [4,6–8,19]. Among the pioneers in the investigation of thermodynamic condensation was Aitken, who observed experimentally in 1880 that any dust or salt particles present in the expansion of saturated air will act as centers for condensation (a heterogeneous condensation). But it was Wilson (1897) who made a detailed study of spontaneous condensation and found that in the absence of ions or foreign nuclei during the expansion of saturated air, condensation was delayed. In the research on spontaneous condensation, attempts were made to define the position of Wilson line more precisely. It was found that the limiting supersaturation was dependent on the nozzle shape and experimental condition and Rettaliata suggested the replacement of the Wilson line by Wilson zone. The Wilson zone includes the supersaturated states in the range of about 3–8% equilibrium wetness line [12].

The liquid phase in the vapor flowing through stages of the steam turbine was the cause of a number of failures. The droplets formed by condensation cause erosion and corrosion of turbine blades by their centrifugal impact and corrosive nature. The newly nucleated droplets are generally too small to cause erosion damage but some of the droplets are collected by the stator and rotor blades to form films and rivulets on the blade and casing walls. On reaching the trailing edges or the tips of the blades, the liquid streams are re-entrained into the flow in the form of coarse droplets. It is these larger droplets that cause the erosion damage. Nowadays, due to work of steam turbines at partial load, process of homogeneous and heterogeneous condensation is still observed. The formation of condensate droplets under conditions other than nominal operation of the turbine is still an unknown process. Engineers and designers involved in the development of power generation machines using condensable working fluids, have a need to

better understand the impact of moisture formation on a machine performance and its lifetime. In meeting this interest, the large-scale experiments and measurements are generally most significant and required if the technical process is to be considered [4,6–8,11,19,20].

The paper focuses on the prediction of the spontaneous condensation phenomena in the wet steam flow depending on the inlet temperature. The basic tests, including comparison with experimental data, have been performed using the planar symmetrical nozzle with the de Laval geometry (IMP PAN nozzle). It was assumed in calculations that steam is very pure and doesn't contain heterogeneous sources of condensation. Numerical analysis was performed for the boundary conditions which correspond to the flow regime without the shock wave. The present work includes simulation results of the onset of condensation and shows whether initiation of a phase transition is located in the region between a spinodal and a binodal. It is assumed that the spinodal (for vapor) corresponds to 8% equilibrium wetness line while the binodal corresponds to the saturation line ('dryness fraction', $x = 1$). Numerical results along the nozzle axis are presented on the thermodynamic diagrams for all considered flow conditions. Additionally, for all considered boundary conditions a maximal subcooled vapor temperature at the place of the beginning of nucleation zone on the nozzle axis is determined.

2 Evolution equation of wetness fraction in single continuum wet steam model

A single continuum wet steam (SCWS) model consists of governing equations which are based on the balance of liquid-vapor mixture. For a consistent non-equilibrium condensation model, a set of nine transport equations can be written in general form

$$\partial_t(\rho\,\phi) + \mathrm{div}(\rho\,\phi\,v) = \mathrm{div}(J_\phi) + \rho\,S_\phi\ , \tag{2}$$

where $\phi = \{1, v\ , e, k, \varepsilon, x,\ a\}$ represents the relevant conserved variable vector. The first three variables come from the well-known equations: balance of mass ($\phi = 1$), balance of momentum ($\phi = v$ – three equations) and balance of energy ($\phi = e$). The additional balance equations for turbulent kinetic energy, turbulent energy diddipation rate, dryness fraction, and interphase surface density are related to the evolution of the turbulence in the condensing flow or the condensation evolution under turbulent flow conditions. Both are fully non-equilibrium phenomena, that should be combined by the sources S, and thermodynamical forces which constitute the fluxes J. The above set of nine equations is to be integrated

within every finite volume. The process of growth of individual droplets is governed by mass, momentum and energy transport mechanisms between the gas and liquid phases. Droplet growth can be described by an evolution of the droplet radius that moves in the wet steam field. The evolution equation of dryness fraction is given by

$$\partial_t(\rho\, x) + \mathrm{div}(\rho\, x\, v) = \mathrm{div}(J_x) + \rho\, S_x\ . \tag{3}$$

The wetness fraction sources, S_x, can be divided into homo- and heterogeneous sources of the mass generation rate due to condensation and evaporation. The homogenous source is given by the sum of mass increase due to nucleation (the formation of critically sized droplets) and also due to growth/evaporation of these droplets

$$S_x = \frac{4}{3}\pi\rho_l \mathrm{I}\mathrm{r}_*^3 + 4\pi\rho_l\, \alpha \bar{\mathrm{r}}^2 \frac{\partial \bar{\mathrm{r}}}{\partial t}\ , \tag{4}$$

where: $\bar{\mathrm{r}}$ – the average radius of droplet ρ_l – density of condensed phase, r_* – the critical radius of droplet, I – the volumetric rate of nucleation [number of droplets/m^3], α – volume fraction of condensate. The expression for r_* is given by

$$\mathrm{r}_* = \frac{2\sigma}{\rho_1 RT \ln S}\ , \tag{5}$$

where σ is the liquid surface tension evaluated at temperature T, ρ_1 is the condensed liquid density (also evaluated at temperature T), R is the universal gas constant, and S is the super saturation ratio defined as the ratio of vapor pressure to the equilibrium saturation pressure. Other details of the SCWS model have been presented in articles [4–6,19,20].

2.1 Interaction of turbulent and phase microstructure

In our approach, the phase microstructure has similar size like the turbulent microstructure which can be evaluated by the following concept: according to possible split of modes of momentum transport only two scalar parameters can describe the evolution of turbulent microstructure, i.e., the turbulent energy k and the turbulent dissipation rate ε. The evolution equation for turbulent microstructure has the following form:

$$\partial_t(\rho\, k) + \mathrm{div}(\rho\, k\, v) = \mathrm{div}(J_k) + \rho\, S_k\ , \tag{6}$$

$$\partial_t(\rho\, \varepsilon) + \mathrm{div}(\rho\, \varepsilon\, v) = \mathrm{div}(J_\varepsilon) + \rho\, S_\varepsilon\ . \tag{7}$$

Transport of non-equilibrium properties between the phase and turbulent microstructure can be described directly on the microstructure level, without exploring the total momentum equation. It may be done by introducing the crossing effects in phase and turbulence fluxes [4–6]:

i. turbulent kinetic energy, k

$$J_k = (D_{kk})\mathrm{grad}k + (D_{kxo} + D_{kxr})\mathrm{grad}x \ , \tag{8}$$

ii. dryness fraction, x

$$J_x = (D_{kxo} + D_{kxr})\mathrm{grad}k + (D_{xxo} + D_{xxr})\mathrm{grad}x \ , \tag{9}$$

iii. turbulent energy dissipation rate, ε

$$J_\varepsilon = (D_{\varepsilon\varepsilon})\mathrm{grad}\varepsilon + (D_{\varepsilon ao} + D_{\varepsilon ar})\mathrm{grad}a \ , \tag{10}$$

iv. interphase surface density, a

$$J_a = (D_{a\varepsilon})\mathrm{grad}\varepsilon + (D_{aao} + D_{aar})\mathrm{grad}a \ . \tag{11}$$

Diffusion coefficients D, which are related with homogeneous diffusion known as the Ostwald mode (subscript o), and heterogeneous condensation mode (subscript r) need estimations and calibrations [4–5,6, 9,20].

3 Validation of single continuum wet steam model by comparison with experimental data

The SCWS model (single continuum approach) with a special microstructure growing up during phase transitions, proposed by Bilicki and Badur [5], was validated on the Institute of Fluid-Flow Machinery, Polish Academy of Sciences (IMP PAN) experiment carried out by Puzyrewski [21]. The experiment was conducted on a symmetric nozzle of 'rectangular' cross-section. The length of the IMP PAN nozzle was 566 mm and its width was 25.2 mm. The nozzle throat (critical throat height of 32 mm) was located 100 mm downstream the nozzle inlet. Details of the nozzle geometry and IMP PAN experiment can be found in [19,21]. The geometry of the nozzle was split into subdomains what enabled creation of a higher quality mesh. Finite volume discretization of the symmetrical planar IMP PAN nozzle is presented in Fig. 2. During the experiment, static pressure measurements were

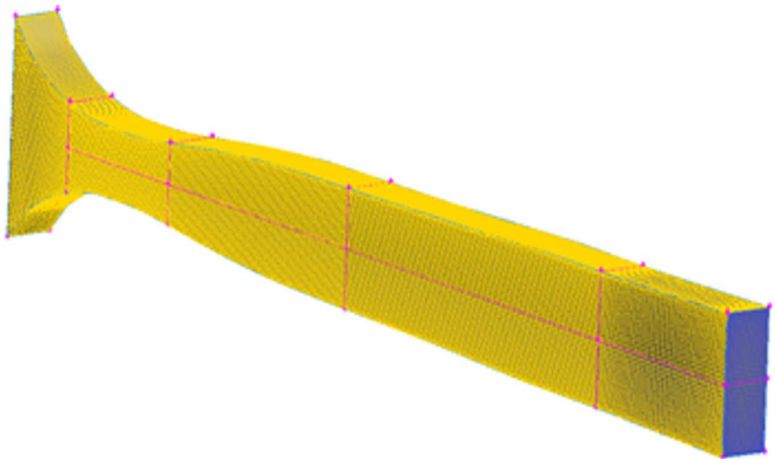

Figure 2: Finite volume discretization of the IMP PAN nozzle.

made on both side walls of the channel. Inlet parameters were close to the saturation line, in order to induce condensation. To validate the computational fluid dynamics (CFD) model, selected boundary conditions corresponding to the Vth set of experimental data were adopted. Details of the experimental measurements can be found in [21].
Figure 3 shows a comparison of the relative static pressure distribution obtained numerically with the experimental data. The SCWS model, describing both condensation and re-vaporization, exhibits a good agreement with the experiment (describes very well the static pressure distribution).

4 Numerical analysis of the onset of two-phase flow in the IMP PAN nozzle

It was assumed in the calculations that steam is very pure and does not contain any heterogeneous sources of condensation. Numerical analysis was performed with boundary conditions corresponding to the flow regime without a shock wave. The entire geometry of the symmetrical nozzle was split into several subdomains what enabled creation of a higher quality mesh. In the first step of simulations it was decided to decrease the grid size only in the zones close to the inlet and to the outlet of the channel. After having determined the position of droplet nucleation in the flow, in the next step an increased grid resolution was applied in these places. Additionally, a decreased size of finite volumes upstream and

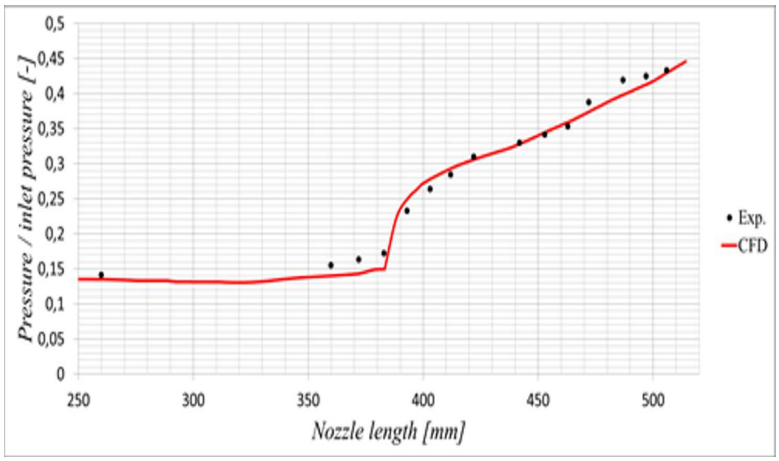

Figure 3: Comparison of the static pressure distribution (related to the inlet pressure) over the nozzle length obtained from CFD calculations solid line) with experimental data (circular points).

downstream of the nucleation zone, about 15 mm in each direction, was applied. When calculation results in the next step were the same (or approximately the same) as in the previous step, they were considered as mesh-independent and mesh refinement was finished. These steps were applied for each considered case with different boundary conditions. Steam temperature in the nozzle axis was monitored during calculations in order to determine the maximal subcooled vapor temperature.

4.1 Boundary conditions adopted to numerical analysis

Two different values of the inlet pressure were assumed in numerical calculations: p_{inlet} = 0.15 MPa and p_{inlet} = 0.7 MPa . For the inlet pressure p_{inlet} = 0.15 MPa, simulations with the nozzle pressure ratio (NPR) p_{inlet}/p_{outlet} = 4.5 were performed. For the bigger value of the inlet pressure, simulation with NPR = 7.7 was conducted. For these two different pressure conditions numerical calculations were performed with various values of the inlet temperature, T_{inlet}. The boundary conditions adopted to the numerical analysis are shown in Tab. 1.

Table 1: Boundary conditions assumed in numerical analysis.

Case	p_{inlet}[MPa]	T_{inlet} [°C]	NPR [–]
A140	0.15	140	4.5
A160	0.15	160	4.5
A180	0.15	180	4.5
A200	0.15	200	4.5
B200	0.70	200	7.7
B220	0.70	220	7.7
B240	0.70	240	7.7
B260	0.70	260	7.7

5 Results and discussion

The position of the nucleation zone mainly depends on the inlet temperature and the purity of steam. The effect of the inlet temperature on the location of the nucleation zone was analyzed by using CFD model in [22], based on the test data. In each case of the steam flow in the IMP PAN nozzle, spontaneous condensation phenomena occurs in the divergent part of the nozzle. For each case of the inlet pressure, the nucleation zone is shifted towards the nozzle entry with decreasing value of the inlet temperature. Calculated wetness fractions for different inlet temperatures and for the inlet pressure of 0.15 MPa and 0.7 MPa are shown in Figs. 4 and 5, respectively. Numerical results are presented in these figures on the plane which crosses the nozzle in the middle of its width (further referred to as a central plane).

For the case with the higher inlet pressure and the same value of the inlet temperature, the nucleation zone occurs earlier (compare Fig. 4d – case A200 with Fig. 5a – case B200). The expansion line for the case with lower inlet pressure is shifted to the right on the enthalpy–entropy diagram. This means that for this case of higher pressure expansion, the saturation line (and thus also the Wilson line) will be crossed. Therefore, the position of the nucleation zone for smaller inlet pressures is shifted to the nozzle exit. In each considered case, the steam enters the nozzle as superheated and leaves it as wet.

Steam expansions lines (obtained from the numerical calculations) on the pressure–volume diagram along the nozzle axis for the inlet pressure 0.15 MPa

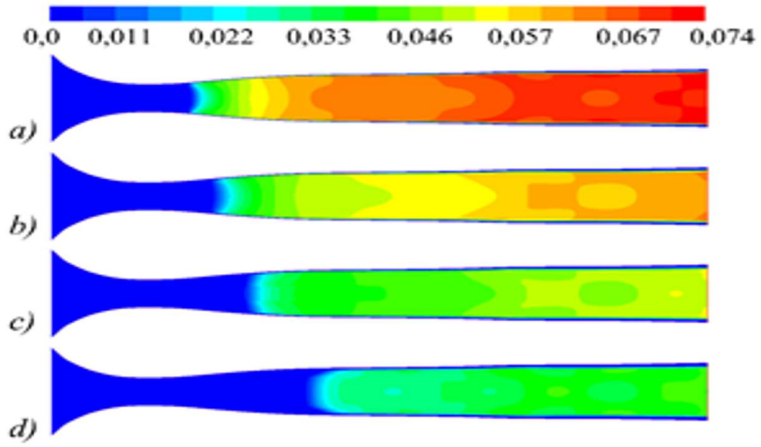

Figure 4: Distribution of the wetness fraction ($y = 1 - x$) on the central plane for the inlet pressure 0.15 MPA and inlet temperatures: a) 140 °C, b) 160 °C, c) 180 °C, and d) 200 °C.

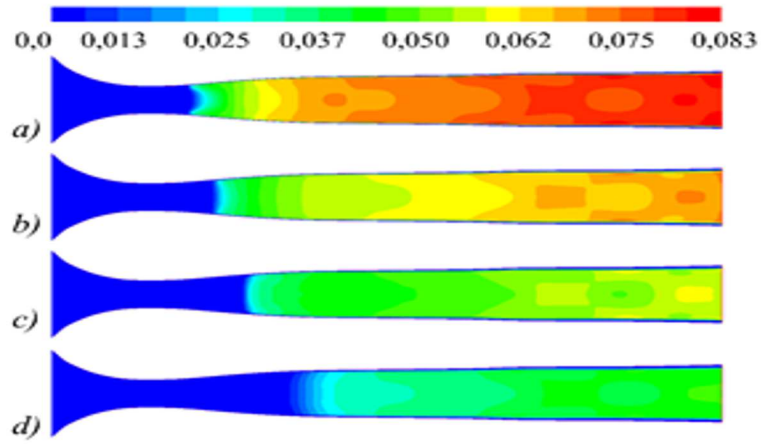

Figure 5: Distribution of the wetness fraction ($y = 1 - x$) on the central plane for the inlet pressure 0.15 MPa and inlet temperatures: a) 200 °C, b) 220 °C, c) 240 °C, and d) 260 °C.

and 0.7 MPa are shown in Figs. 6 and 7, respectively. Regardless of the boundary conditions, for all considered cases there exists higher or smaller peak of the pressure, which determines the onset of condensation. The nucleation process leads to the formation of very large number of tiny droplets, called the primary fog, more or less uniformly distributed in the continuous vapor phase. The droplets

formed in such a way rapidly grow by exchanging heat and mass with the surrounding subcooled vapor [10]. The high rate of heat release as a result of rapid condensation, causes a sharp increase in a vapor temperature and consequently an exponential decay of the subcooling. Depending on the values of the flow parameters, the initial growth phase of the droplets may give rise to a gradual increase in pressure known as condensation shock.

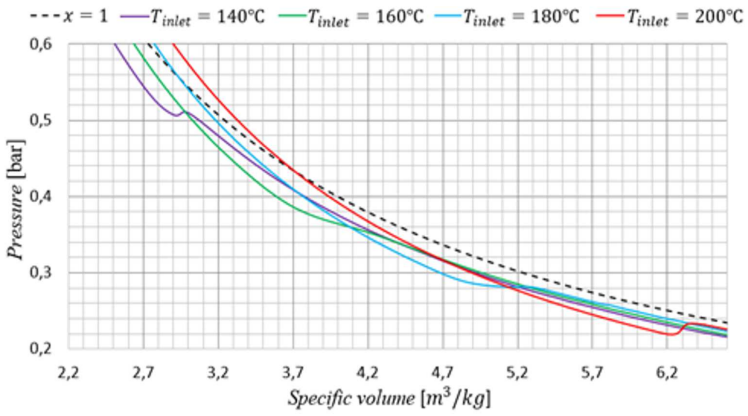

Figure 6: Steam expansion on pressure–volume diagram along the nozzle axis for the inlet pressure 0.15 MPa and different values of the inlet temperature.

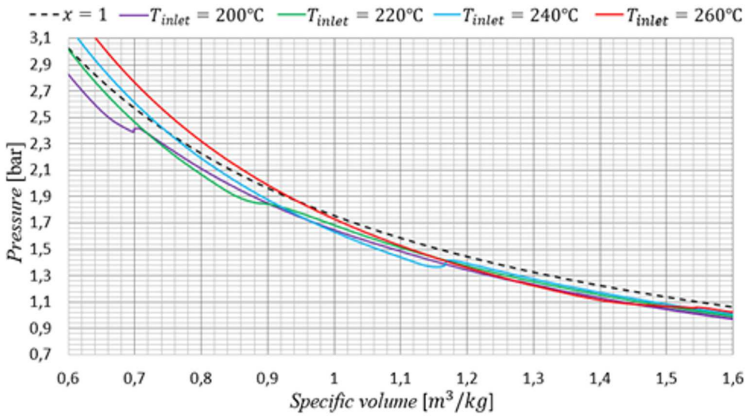

Figure 7: Steam expansion on pressure–volume diagram along the nozzle axis for the inlet pressure 0.7 MPa and different values of the inlet temperature.

Figures 8 and 9 present the numerically calculated steam expansion lines along the nozzle axis on the Mollier enthalpy–entropy diagrams for the inlet pressure of 0.15 MPa and 0.7 MPa, respectively. For each case of the inlet pressure, the expansion line on the chart is shifted to the left with decreasing value of the inlet temperature. For each considered case, the steam expansion in the IMP PAN nozzle is approximately isentropic to the state when the steam reaches the saturation line. After crossing the saturation line, the steam entropy increases due to supercooling, metastable state, very high velocity (supersonic flow) and shock condensation until reaching the Wilson line. In each considered case, the Wilson line (onset of condensation) is achieved for approximately 0.97 equilibrium dryness fraction line. The phase change induces the latent heat release, so that the flow comes back to the equilibrium condition. Expansion of the flow downstream the Wilson line takes place close to equilibrium conditions and in each case is approximately isentropic.

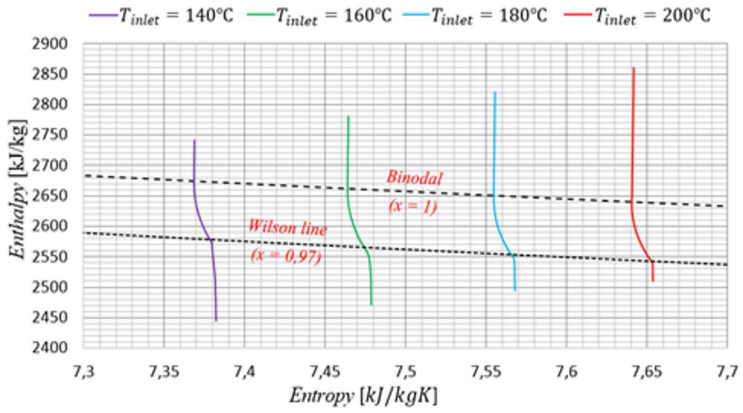

Figure 8: Change of the steam entropy during the expansion for the inlet pressure of 0.15 MPa and different inlet temperatures.

Table 2 presents numerical results for the maximum wetness fraction, y, the maximum level of vapor supercooling, ΔT, and the value of the Wilson point (defined as a value of the equilibrium dryness fraction at the onset of non-equilibrium condensation) x for all considered cases of boundary conditions. In all cases, with increasing the inlet temperature, the maximum wetness fraction decreases but the level of vapor supercooling increases. The supercooling is within the range from 26.8 °C (case B200) to 36.89 °C (case A200) which is consistent with the theory and experimental measurements. With increasing the inlet pressure, the

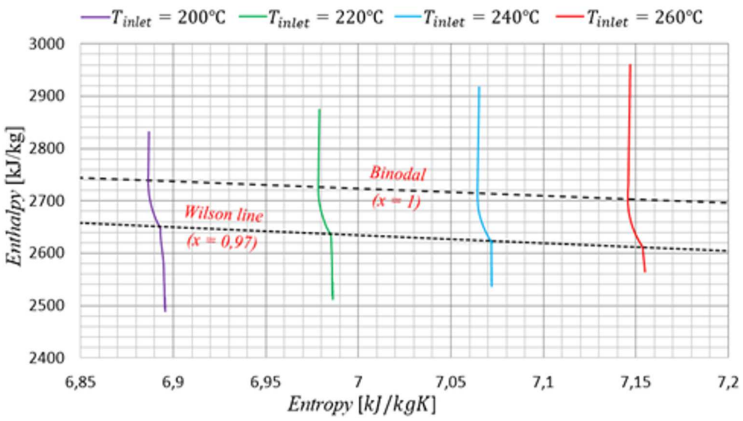

Figure 9: Change of the steam entropy during the expansion for the inlet pressure of 0.7 MPa and different inlet temperatures.

supercooling decreases (compare case A200 with B200). For all considered cases of boundary conditions, the Wilson point is reached at the point of approximately 3% equilibrium wetness fraction.

Table 2: Numerical results of maximum wetness fraction, y, maximum level of vapor supercooling, ΔT, and a value of the Wilson point, x.

Case	y [–]	ΔT [°C]	Wilson point (x [–])
A140	0.0742	33.24	0.9713
A160	0.0610	33.35	0.9690
A180	0.0497	35.07	0.9715
A200	0.0392	36.89	0.9712
B200	0.0831	26.80	0.9717
B220	0.0691	27.89	0.9705
B240	0.0564	31.70	0.9713
B260	0.0426	28.74	0.9725

6 Conclusions

In this paper, the initiation of the phase transition (onset of condensation called the spontaneous condensation phenomenon) in the IMP PAN nozzle depending on the inlet temperature was analyzed for experimental cases without the shock wave in the steam flow. The non-equilibrium single continuum wet steam model with a special microstructure developing during phase transition was validated by the experiment carried out by Puzyrewski on the planar symmetrical de Laval nozzle. The numerical results obtained using the model agree fairly well with the experimental data (pressure distribution along the nozzle walls for Vth set of experimental conditions). Additionally, for all considered boundary conditions the level of subcooled vapor temperature and the Wilson point were determined.

The performed numerical investigations have shown that:

1. When pure steam expands in a nozzle or a turbine blade passage, droplets do not appear as soon as the condition line crosses the saturation line, and therefore the spontaneous condensation is a non-equilibrium phase transition process. For some considerable time during expansion, the steam remains dry in a metastable equilibrium until the subcooling becomes high enough to trigger a considerable nucleation rate.

2. The initial phase of the droplets growth may give rise to a gradual increase in pressure known as condensation shock.

3. The position of the nucleation zone depends on the inlet temperature and pressure. The nucleation zone is shifted to the nozzle entry with decreasing value of the inlet temperature.

4. For the case with higher inlet pressure and the same value of the inlet temperature, the nucleation zone occurs earlier.

5. Independently of the boundary conditions, for all considered cases there exists a larger or smaller pressure peak determining the onset of condensation (pressure volume diagrams).

6. For each case of boundary conditions, the Wilson line (beginning of the condensation) is achieved for approximately 0.97 equilibrium dryness fraction line which agrees with the theory and experiments.

7. In all cases of the inlet pressure, with increasing the inlet temperature the maximum wetness fraction decreases, but the level of vapor supercooling increases.

8. The supercooling is within the range from 26.8 °C to 36.89 °C which is consistent with the theory and experimental measurements.

9. For all considered cases of boundary conditions, the Wilson line is reached at approximately 3% equilibrium wetness line.

All calculations were performed with the assumption that steam is chemically pure but it is not known what will happen in the case heterogeneous sources of condensation are present. Therefore, development of models for condensation and evaporation is still necessary. As most of the experimental data used for validation of the numerical models are relatively old, new experimental measurements employing modern measuring techniques are required.

Received in June 2017

References

[1] Yang Y., Shen S.: *Numerical simulation on non-equilibrium spontaneous condensation in supersonic steam flow.* Int. Commun. Heat Mass Transfer **36**(2009), 902–907.

[2] Gerber A.G., Kermani M.J.: *A pressure based Eulerian–Eulerian multi-phase model for non-equilibrium condensation in transonic steam flow.* Int. J. Heat Mass Transfer **47**(2004), 2217–2231.

[3] Nag P.K.: *Power plant engineering.* Tata McGraw-Hill, New Delhi 2008.

[4] Kornet S., Badur J.: *Partial evaporation and total cut-off wet steam region on the shock wave.* In Proc.: 3rd Polish Cong. of Mechanics and 21st Int. Conf. on Computer Methods in Mechanics, Short Papers vol. 2, Polish Society of Theoretical and Applied Mechanics, 2015, 523–524.

[5] Bilicki Z., Badur J.: *A thermodynamically consistent relaxation model for a turbulent, binary mixture undergoing phase transition.* J. Non-Equilibrium Thermodyn. **28**(2003), 2, 145–172.

[6] Kornet S., Badur J.: *Enhancement evaporation of the condensate droplets within the asymmetrical shock wave zone.* Trans. Inst. Fluid-Flow Mach. **128**(2015), 119–130.

[7] Dykas S., Majkut M., Smołka K., Strozin M.: *Research on steam condensing flows in nozzles with shock wave.* J. Power Technolog. **93**(2013), 5, 288–294.

[8] Puzyrewski R.: *Theoritical and experimental studies on formation and growth of water drops in LP steam turbines.* Trans. Inst. Fluid-Flow Mach. **42-44**(1969), 289–303.

[9] Chang Hyun Kim C. H., et al.: *Numerical analysis of non-equilibrium steam condensing flows in various Laval nozzles and cascades.* Eng. Appl. Comput. Fluid Mech. **11**(2017), 1, 172–183.

[10] Guha A.: *Analysis and computation of non-equilibrium two-phase flows.* Sâdhanâ **22**(1997), **3**, 295–321.

[11] Sanju Hosur H., Anjaneyulu, Muralidharan K.V.: *Numerical study on homogenous condensation of steam in converging diverging nozzle*. Int. J. Res. Eng. Technol. **5**(2016), 9, 44–47.

[12] Wegener P. P., Mack L.M.: *Condensation in supersonic and hypersonic wind tunnels*. Adv. Appl. Mech. **5**(1958), 307–447.

[13] Gyarmathy G.: *Grundlagen einer Theorie der Nassdampfturbine*. Institut fur Termische Turbomaschinen, Zurich 1962.

[14] Puzyrewski R., Król T.: *Numerical analysis of Hertz-Knudsen model of condensation upon small droplets in water vapor*. Trans. Inst. Fluid Flow Machinery **70-72**(1976), 285–308.

[15] Stodola A.: *Undercooling of Steam Through Nozzle*. Engineering (1915), 643–646.

[16] Wróblewski W., Dykas S., Gardzilewicz A., Kolovratnik M.: *Numerical and experimental investigation of steam condensation in LP part of large power turbine*. J. Fluids Eng.-T ASME, **131**(2009), 4, 1–11.

[17] Kornet S., Badur J.: *Comparison of two models of condensation*. PhD Int. J. **1**(2014), 193–203.

[18] Rajadurai J. S.: *Thermodynamics and Thermal Engineering*. New Age Int. (P), New Delhi 2003.

[19] Kornet S., Badur J.: *An asymmetrical λ-foot of condensing steam flow in the IMP PAN nozzle. J. Phys.: Conf. Ser.* **530**(2014), 012018, 1–8.

[20] Kornet S., Badur J.: *"Eulerian – Eulerian" versus „Eulerian –Lagrangean" models of condensation*. Logistyka **4**(2014), 4463–4473.

[21] Puzyrewski R., Gardzielwicz A., Bagińska M.: *Shock wave in condensing steam flow through a Laval nozzle*. Arch. Mech. **25**(1973), 3, 393–409.

[22] Chandler K., Melas M., Jorge T.: *A study of spontaneous condensation in an LP test turbine*. ASME Turbo Expo 2015: Turbine Tech. Conf. Exposition, Montreal 2015.